

Received December 30, 2019, accepted January 9, 2020, date of publication January 20, 2020, date of current version February 5, 2020.

Digital Object Identifier 10.1109/ACCESS.2020.2968052

# Comparative Study of Compressed Sensing for Heart Sound Acquisition in Wireless Body Sensor Networks

SHUANG SUN<sup>1</sup>, JIAZHU XING<sup>1</sup>, ZHENG ZHOU<sup>2</sup>, WEI WANG<sup>2</sup>, (Member, IEEE),  
AND JUNXIN CHEN<sup>1,2</sup>

<sup>1</sup>College of Medicine and Biological Information Engineering, Northeastern University, Shenyang 110004, China

<sup>2</sup>Department of Computer and Information Science, University of Macau, Taipa, Macau

Corresponding author: Junxin Chen (chenjx@bmie.neu.edu.cn)

This work was supported by the National Natural Science Foundation of China under Grant 61802055 and Grant 61771121.

**ABSTRACT** With the application of wireless body sensing network to real-time monitoring of biological signals, compressed sensing (CS) has become a promising signal acquisition technology that can extend monitoring time, reduce equipment cost and decrease power consumption. This paper makes a comparative study on the acquisition of heart sound (HS) signals by CS, compares and analyzes the performance of wavelet basis, reconstruction algorithms and frames. Among a large number of experimental data records, the reconstruction performance under different compression rates is comparatively studied, and the suitable wavelet basis, reconstruction algorithm and signal frame size for HS acquisition are obtained. The presented performance records and comparative analyses can give benchmarks for future academic research, and are also believed to be beneficial for practical applications.


**INDEX TERMS** Compressed sensing, heart sound, wavelet basis, reconstruction algorithm.

## I. INTRODUCTION

According to the report of World Health Organization, cardiovascular diseases (CVDs) are the number one cause of worldwide death, an estimated 31% of all the deaths globally. In a single year of 2017, the CVDs are responsible for approximately 17.8 million deaths [1]. Individuals at risk of CVDs usually have irregular blood pressure, heart rate, etc., which are generally easier to be monitored. In this scene, long-term and real-time monitoring of body status plays critical roles for earlier diagnosis and better treatments of the CVDs. The rapid developing wireless body sensor network (WBSN) emerges as a promising solution [2]. The WBSN's sensors first collect the biomedical signals of a patient, then transmits these parameters to a remote center which always locates in a hospital. Finally, with the state-of-the-art analysis by the artificial intelligent and medical diagnosis, the CVDs can be earlier discovered and better treated. In addition, WBSN can also be integrated as a sub-network into Internet-connected networks or Internet of Things [3], [4] and provide various

smart healthy services, as demonstrated in Fig. 1. Benefiting from the remarkable progresses of wearable devices and networking technologies [5]–[7], WBSN is expected to play more important roles for intelligent health treatments in the future smart cities. For the acquisition process of WBSN, energy consumption of the sensors is the most critical problem for practical applications [8]–[10], because it has remarkable impacts to prolong the monitoring time and to make the devices smaller and comfortable. The traditional signal acquisition techniques are based on Nyquist-Shannon theory. They require high energy consumption, and further result in the high cost of the sensors [11], [12]. Improving the signal acquisition and processing method in terms of energy consumption is of great significance for extending the lifespan of bio-sensors, and thus prolong the monitoring time of the WBSN for collecting the patient's healthy parameters.

Compressed sensing (CS) is a new signal acquisition technology with the advantage of low power consumption [13]. Based on the sparse characteristics of the signals, CS is able to reconstruct the original signal with less sampled data [12]. Compared with the traditional Shannon's theorem, the lower sampling frequency will remarkably reduce the

The associate editor coordinating the review of this manuscript and approving it for publication was Liangtian Wan .

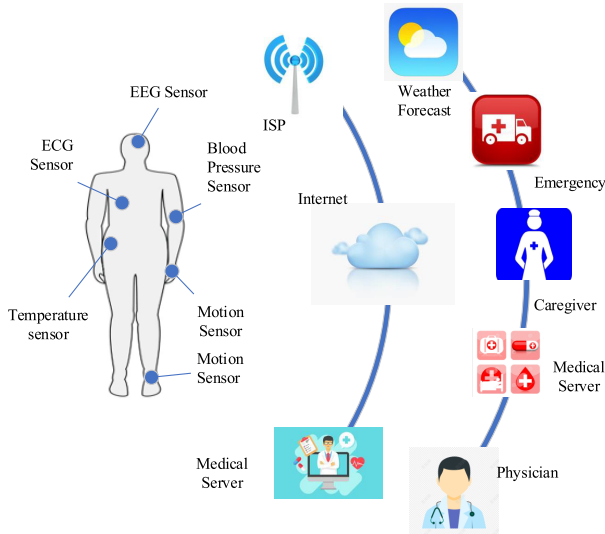


FIGURE 1. Illustration of the wireless body sensor network.

energy consumption. At the same time, CS can compress the signal in the process of acquisition, so as to reduce the data volume and achieve the purpose of reducing data storage and power consumption [12], [14]. At present, CS has been widely used for signal acquisition and processing [15]–[18]. When applied in WBSN, CS can significantly improve the monitoring efficiency of the bio-sensors and furthermore extend the monitoring durations [8], [19]. It has been proposed by Zhang *et al.* [20] and Polania and Barner [21] that using CS for electrocardiograph (ECG) signals had good reconstruction quality and can be well applied to the design of WBSN. In [22], Zhang *et al.* proposed the block sparse bayesian learning (BSBL) algorithm for reconstructing ECG signals from the CS measurements, and demonstrated that BSBL had remarkable advantages over traditional solutions in terms of accuracy and efficiency. On the other hand, Pant and Krishnan [23] analyzed the reconstruction performance of CS for different QRS complexes, and concluded that the reconstruction performance of CS is related to specific QRS. By promoting the sparsity of ECG on the first-order and second-order difference, reconstruction algorithms based on  $l_p^d$  and  $l_p^{2d}$  optimization are theoretically investigated and experimentally validated in [19]. In addition, applications of CS for acquiring electroencephalogram (EEG) [24] and electromyography (EMG) [25] were also investigated.

On the other hand, researchers seldom explored CS for sampling heart sound (HS) signals. In addition to ECG, HS is also an important reference for monitoring CVDs. Sejdic and Chaparro [26] had proven that CS is suitable for acquiring HS, and demonstrated that 40% samples are sufficient to reconstruct the original HS signals accurately. Cheng *et al.* [27] proposed and verified a multi-channel CS model for HS acquisition. The achievements of [26] and [27] fully proved that the CS is suitable for the reconstruction of heart sound signal. However, extensive study of CS for

HS acquisition is lacking at present. The aforementioned related works didn't give the most suitable benchmarks for HS reconstruction in terms of the common-used wavelet basis, reconstruction algorithms and frame sizes. The academic research requires benchmarks, and the practical applications also need referred data records.

In this work, we conduct a comparative analysis on the acquisition of HS using CS technique. A total of 52 wavelet basis, 5 reconstruction algorithms are introduced, and the impact of frame size is also evaluated. The contributions of this paper can be summarized as follows.

- 1) The acquisition of heart sound using CS technique has been compressively analyzed.
- 2) Different wavelet basis have been tested, and the best sparse basis which can serve as benchmarks for future sparsifying basis has been found out.
- 3) Various reconstruction algorithms have been analyzed, the results can serve benchmarks for future recovery techniques.
- 4) This paper first investigates the effect of frame size for the reconstruction of HS signals.
- 5) The source sources are open accessible for extension.<sup>1</sup>

The remainder of this paper is organized as follows. Section II introduces the basic theory of CS and HS, and also sketches the application of CS for HS acquisition. The experiment configuration is given in Section III, while the results are described and analyzed in Section IV. Finally, conclusions will be drawn in the last section.

## II. RELATED WORK

### A. COMPRESSED SENSING

As introduced in [12], [13], [20], [23], CS is a technology that uses fewer samples (than those in Nyquist-Shannon theorem) to reconstruct the original signal. As long as the signal is sparse or compressible in certain transform basis, the CS theory demonstrates that it can be acquired by a linear sampling process and then reconstructed by optimization approaches. The classical sparse transform methods include discrete cosine transform, Fourier transform, discrete wavelet transform, etc [12], [13], [28].

Mathematically, let signal  $x$  be a one-dimensional signal of length  $N$ , and the sparsity is  $k$  ( $k \neq 0$ ). The signal  $x$  can be sparsely expressed as

$$\mathbf{x} = \Psi \mathbf{s} \tag{1}$$

where  $\Psi$  is the sparse basis matrix and  $\mathbf{s}$  is the coefficient. A suitable sparse transform should be selected to minimize the number of the non-zero coefficients, i.e., to promote the sparsity level. When the signal can be represented sparsely, a random measurement matrix  $\Phi$  is employed to project the high-dimensional signal onto the a low-dimensional space, and get the measurement vector  $\mathbf{y}$  as

$$\mathbf{y} = \Phi \mathbf{x}, \tag{2}$$

<sup>1</sup>The source codes are open accessible via [https://github.com/lurenjia212/CS\\_Heart\\_Sound\\_Acquisition/](https://github.com/lurenjia212/CS_Heart_Sound_Acquisition/).

where  $\Phi$  is with dimension  $M \times N$ . In this scene, the  $N$ -dimensional signal  $x$  has been compressively sampled as an  $M$  dimensional measurement  $y$ . Combining Eqs. (1) and (2), the CS acquisition process is finalized into Eq. (3) in which  $\Theta$  denotes sensing matrix.

$$\mathbf{y} = \Phi \mathbf{x} = \Phi \Psi \mathbf{s} = \Theta \mathbf{s}. \quad (3)$$

Only when matrix  $\Theta$  satisfies the Restricted Isometry Property (RIP) [29], the  $M$ -dimensional measured value  $y$  can preserve sufficient information for fully recovering the original signal  $x$ . The equivalent condition of RIP is that the measurement matrix  $\Phi$  is unrelated to the sparse basis. This property ensures that the measurement matrix will not map two different  $K$  sparse signals into the same set. It has been proven that Gaussian matrix, Bernoulli matrix, Fourier random matrix, Hadamar matrix are unrelated to the common-used sparse basis, and thus guarantee the RIP of the resultant  $\Theta$ . In other words, these random matrices can be used as the alternative measurement matrix of CS.

Unlike the linear multiplication in the acquisition process, signal reconstruction should be preformed with the help of optimization approaches. The reconstruction process is

$$\min \|\mathbf{s}\|_1 \quad \text{subject to } \mathbf{y} = \Theta \mathbf{s}. \quad (4)$$

After obtaining  $\mathbf{s}$ , the the signal is further calculated by Eq. (1). The current commonly used algorithms for Eq. (4) can be roughly divided into convex optimization, greedy pursuit, and iterative thresholding. In specific, the widely-used reconstruction algorithms include Orthogonal Matching Pursuit (OMP), Basis Pursuit (BP), Compressive Sampling Matching Pursuit (CoSaMP), iteratively reweighted least squares (Irls), and subspace pursuit (SP) [12], [22], [30]. The performance of these reconstruction algorithms for ECG acquisition has been investigated in [8]. These algorithms will also be adopted in this work.

## B. HEART SOUND SIGNALS

The HS signals are the sounds when our hearts contract. They are periodic signals that can be recorded by a stethoscope or special electronic instrument. The pathological state of the heart is distorted, resulting in the noise of the HS. Doctors can make the initial diagnosis through the noise or a series of medical indicators including heart rate, heart sounds, duration of diastolic and systolic events (W1/W2), and diastolic and systolic periods (D/S) [31]. As an important indicator of CVDs, heart sound signal has an many advantages. The HS has characteristics of non-originality and good periodicity, and the presence of murmur or distortion in HS reveals the cardiovascular diseases. The application of HS for detecting CVDs has received increasing attention in recent years.

The periodic beating of the heart produces four heart sounds: the first (S1), the second (S2) (normally heard), the third (S3 is usually heard only by children and adolescents), and the fourth (S4 is rarely heard normally) [26], [32], as shown in Fig. 2.

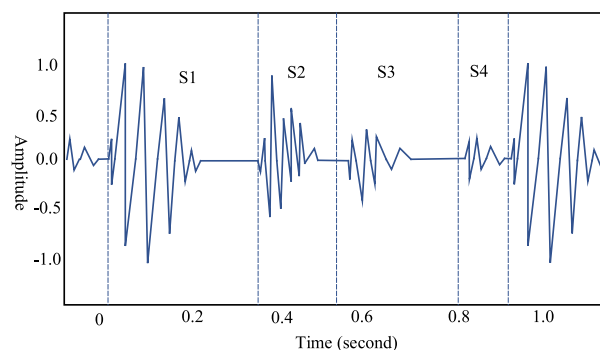


FIGURE 2. Illustration of a HS waveform.

The ideal-heart sound has no periodic variation waveform of S3 and S4. Each heartbeat period has two extremes, corresponding to the peaks of S1 and S2. The systolic period of the heart lasts from S1 to S2, and the diastolic period lasts from S2 to S1. Normally, diastole is slightly larger than systole [27]. When the heart beats too fast, diastolic periods shorten, and further make the systolic and diastolic periods identical. The doctors can use this phenomenon to make a diagnosis. According to the different stethoscope area, the intensity of HS will also be different. The S2 signal of aortic area is strong, and the S1 signal of bicuspid valve and tricuspid valve stethoscope area is strong [27]. For the waveform of a group of HS, the three values S1/S2, W1/W2 and D/S obtained by medical indicators can determine the congestive state of the heart [33].

The accuracy and reliability of heart signals determine a doctor's diagnosis. With the development of WBSN, the accuracy and reliability of electronic devices for HS monitoring have been greatly improved, which can be fully applied to the diagnosis of CVDs in clinical treatments.

## C. CS FOR HS ACQUISITION

In comparison with the extensive research on ECG and EEG acquisition, there are few previous works focusing on acquiring HS using the CS technique [26], [27].

There are two previous works can be referred [26], [27]. On one hand, Sejdic and Chaparro [26] first investigated the feasibility of using CS to acquire the HS signals. Based on modulated discrete prolate spheroidal sequences, it was reported that when the measurements have only 40% samples of the original HS signal, the HS can also be accurately reconstructed. On the other hand, Cheng *et al.* [27] proposed a multi-channel model to parallelly collect and compress the HS of different intensity in different auscultation areas. Numerical experimental results demonstrated that the model proposed in [27] was able to achieve a speed of 9-10 times faster than BSBL algorithm, and obtained a better reconstruction quality at the same time.

However, a comprehensive study on CS acquisition of HS signals with common sparsifying basis and reconstruction algorithms is still lacking. The benchmarks in various aspects

require more numerical support. For example, the BSBL is originally developed for ECG acquisition [22] yet it is introduced in [27] as a compared algorithm. If we can use open accessible HS data sets, and find the most suitable sparsifying basis and reconstruction algorithm from the common candidates, then they can be referred as benchmarks in the future academic research. This is our primary concern.

### III. COMPARATIVE EXPERIMENTS

In this work, three factors are evaluated for the HS acquisition with CS technique. Specifically, the wavelet basis, reconstruction algorithms and different frame sizes are tested in terms of various performance indicators. The primary goal is to find the suitable sparsifying basis among wavelet family, the satisfactory reconstruction algorithms among the widely-used ones, and the suitable frame size. The raw data and analytical conclusion are expected being beneficial to not only future academic research but also practical applications.

#### A. PLATFORM AND DATABASE

All of the experiments are implemented by Matlab 2018a on our computing platform, a personal computer with an Intel(R) Core(TM) i7 CPU (3.00 GHZ) and 16 GB memory.

The HS samples in the experiments are obtained from the PhysioNet Database.<sup>2</sup> All the introduced records are first re-sampled to 1024 Hz (from 2048 Hz) and a total of 100 heart sound signals are employed in our experiments.

#### B. PERFORMANCE METRICS

The experiments mainly compares the compression ratio (CR) and reconstruction quality. Three metrics in terms of reconstruction quality are introduced, i.e., percentage root-mean-squared difference (PRD) [8], structural similarity index (SSIM) [13] and executive time. The CR in this paper is defined as

$$CR = 1 - \frac{M}{N}.$$

Obviously, CR is a float number less than 1. The value of CR reveals the length of the samples (measurements).

The PRD is defined as the percentage of distortion between the original signal and the reconstructed signal. The mathematical formula of PRD is

$$PRD = \frac{\|\hat{X} - X\|}{\|X\|} \cdot 100,$$

where  $X$  is original signal and  $\hat{X}$  is reconstructed signal.

The third performance index is SSIM, defined as

$$SSIM(x, \hat{x}) = \frac{(2\mu_x\mu_{\hat{x}} + c_1)(2\sigma_{x\hat{x}} + c_2)}{(\mu_x^2 + \mu_{\hat{x}}^2 + c_1)(\sigma_x^2 + \sigma_{\hat{x}}^2 + c_2)},$$

where  $\mu_x$  is the average of the  $x$ ,  $\mu_{\hat{x}}$  denotes the average of the  $\hat{x}$ ,  $\sigma_x^2$  is the variance of  $x$ ,  $\sigma_{\hat{x}}^2$  is the variance of  $\hat{x}$ ,

<sup>2</sup>The dataset is available via <https://physionet.org/content/challenge-2016/1.0.0/>. We use the data records in *training* - a directory.

while  $\sigma_{x\hat{x}}$  refers to the covariance of original signal and reconstructed signal, respectively. The variable  $c_1$  and  $c_2$  are constant, in our experiment, they are set as  $c_1 = 0$ ,  $c_2 = 0$ . Essentially, SSIM denotes the similarity of two signals, higher SSIM refers to higher similarity.

In addition, the reconstruction time is of course also an important comparison index.

#### C. COMPARATIVE DIMENSIONS

Three factors are included for comparative analysis. The first factor is the sparsifying basis. This paper aims to make a comparative analysis of the reconstruction quality in different wavelet basis, and will give empirical results for future research of HS acquisition. A total of 52 wavelet basis are compared in this work, they are haar, dbn ( $n = 2-10$ ), symn ( $n = 2-8$ ), coifn ( $n = 1-5$ ), biornr.nd ( $nr = 1, nd = 1, 3, 5; nr = 2, nd = 2, 4, 6, 8; nr = 3, nd = 1, 3, 5, 7, 9; nr = 4, nd = 4; nr = 5, nd = 5; nr = 6, nd = 8$ ) and rbionr.nd ( $nr = 1, nd = 1, 3, 5; nr = 2, nd = 2, 4, 6, 8; nr = 3, nd = 1, 3, 5, 7, 9; nr = 4, nd = 4, nr = 5, nd = 5; nr = 6, nd = 8$ ).

The second factor is the reconstruction algorithm. When the sensing matrix  $\Theta$  satisfies RIP, the signal  $x$  can be recovered from the  $M$ -dimensional projection  $y$  by a reconstruction algorithm. In our experiments, the measurement matrix is fixed as Bernoulli matrix which can assure the RIP requirements of  $\Theta$  when collaborating with the common-used sparsifying basis. The adopted reconstruction algorithms in our experiments include OMP, BP, CoSaMP, Irls and SP. These algorithms are employed on each CR region.

The last factor is the frame size. A frame is named for the short-time signal which is reconstructed one time. The size of a frame may affect the reconstruction performance in terms of PRD and SSIM [34]. This paper discusses the relationship between the frame size and reconstruction quality. The tested frame sizes include 256, 512, 768, 1024, 2048 and 4096. On the basis of a fixed reconstruction algorithm and measurement matrix, 100 heart sounds were employed to exploit the influence of frame size to the quality of the reconstructed signal. Finally, we suggest the empirical satisfactory frame size for the CS application of HS acquisition.

## IV. RESULTS AND DISCUSSIONS

#### A. PERFORMANCE ANALYSIS VERSUS WAVELET BASIS

First, the reconstruction is implemented over 52 types of wavelet basis. The reconstruction algorithm is fixed as BP, while the frame size is 1024. The experimental results are shown in Tables 1 and 2, and Fig. 3. With the reduction of CR, PRD decreases significantly, i.e., the signal quality improves. The results demonstrate that rbio5.5 is always the best wavelet basis for HS reconstruction. In addition, bior2.6, bior2.8 and rbio4.4 also have good PRD performances. When CR is less than 35%, bior2.6 has a satisfactory reconstruction performance. On the other hand, bior2.8 and rbio4.4 are good choices when CR is in the range of 30%-70%, while bior2.8 is also a good alternative when CR is greater than 70%.



TABLE 1. PRD of various wavelet basis.

Wavelet	10%	20%	30%	40%	50%	60%	70%	80%	90%
hear	8.6369	14.4911	20.6307	28.3235	36.4335	46.1747	58.1768	71.3833	87.0691
db2	6.1418	10.8409	16.4196	23.6786	31.0068	41.2011	53.4448	67.6051	84.6928
db3	5.4270	9.8689	14.7760	21.9065	29.8001	39.7362	52.4105	66.5163	83.6598
db4	5.0687	9.3149	14.3864	21.6799	29.0862	38.6466	51.9005	66.4629	84.5530
db5	5.1130	9.2070	14.1323	21.2607	28.8981	39.0961	51.5463	66.3932	84.6093
db6	4.9121	8.9636	14.1722	20.9448	28.7945	38.8178	52.0242	66.4380	84.2053
db7	4.9032	8.9213	13.9562	21.0288	28.7271	38.8261	51.8571	66.6971	84.4036
db8	4.9292	8.9487	13.9216	21.0637	28.4671	38.7692	51.5136	66.7651	85.2784
db9	4.8440	8.9156	14.0732	21.0384	29.1514	39.0922	52.0624	67.0895	84.9954
db10	4.8783	8.8347	14.1532	21.1667	29.1169	39.1628	52.4903	67.0734	84.7321
sym2	6.1418	10.8409	16.4196	23.6786	31.0068	41.2011	53.4448	67.6051	84.6928
sym3	5.4270	9.8689	14.7760	21.9065	29.8001	39.7362	52.4105	66.5163	83.6598
sym4	5.0711	9.2842	14.3688	21.1855	28.6856	38.2307	51.1979	65.6017	83.1736
sym5	4.9373	9.1054	14.0641	20.8699	28.4901	38.5962	50.9965	66.0807	83.8048
sym6	4.8275	9.0050	14.1141	20.5693	28.0721	37.8767	50.5594	65.6531	83.0509
sym7	4.8560	8.8383	13.7668	20.5812	28.2524	38.0063	50.7885	65.7631	84.0181
sym8	4.7888	8.8683	13.9090	20.4808	27.9666	37.9457	50.3173	65.5962	82.9568
coif1	6.0984	10.7043	16.0608	23.2809	30.8675	40.4641	52.7954	67.1339	83.8902
coif2	5.1213	9.3039	14.1916	21.1033	28.6330	38.5893	51.2339	65.6980	83.0472
coif3	4.9521	8.9684	13.6472	20.6467	28.2414	38.1708	50.6092	65.6759	82.8934
coif4	4.8305	8.7973	13.6068	20.4420	27.9042	37.9310	50.3488	65.6544	83.0959
coif5	4.7226	8.6141	13.5142	20.3551	27.8861	38.0458	50.4126	65.6818	83.3363
bior1.1	8.6369	14.4911	20.6307	28.3235	36.4335	46.1747	58.1768	71.3833	87.0691
bior1.3	4.6242	8.52537	12.9455	19.7531	26.9379	36.5560	49.5242	63.7323	82.6675
bior1.5	4.3536	8.0678	12.7557	19.4521	26.5008	36.1900	48.8379	62.9186	81.9564
bior2.2	7.0293	12.2731	19.4007	28.0587	37.3148	48.1681	60.7478	73.4593	86.8019
bior2.4	4.8270	8.7359	14.2276	21.1592	29.0351	38.9882	51.1366	64.8049	81.2521
bior2.6	4.3001	7.8744	12.8056	19.3636	26.6812	36.5350	48.5854	62.5942	79.8614
bior2.8	4.0916	7.5827	12.3081	18.6627	26.0430	35.7636	47.6263	61.7826	79.2918
bior3.1	16.9649	30.2834	46.0243	64.4826	82.7845	100.5082	116.0555	125.7300	128.3656
bior3.3	6.9252	13.6531	22.3801	34.7910	48.8867	63.5920	78.1791	89.5257	98.6177
bior3.5	5.5337	11.1701	18.4753	29.0765	40.5529	53.8669	67.0728	78.4356	89.6479
bior3.7	5.0779	10.0086	16.9130	26.8672	37.4034	49.8346	62.3661	74.5598	87.1084
bior3.9	4.8539	9.5113	16.1276	25.0821	35.6343	47.9689	60.0981	72.5813	86.1269
bior4.4	6.6415	12.0239	18.8677	26.9836	35.2278	45.4002	57.6769	71.2813	86.2659
bior5.5	9.5453	16.9264	25.7317	36.2334	45.8068	57.1656	70.4478	82.4786	93.9004
bior6.8	5.0800	9.2893	14.5274	21.1504	28.7288	38.5583	51.1609	65.5736	82.6268
rbio1.1	8.6369	14.4911	20.6307	28.3235	36.4335	46.1747	58.1768	71.3833	87.0691
rbio1.3	10.4109	17.4939	24.9673	33.8504	42.7458	52.5480	64.0228	75.9449	89.4436
rbio1.5	10.9918	18.6473	26.5844	35.9870	45.4875	55.2776	66.6827	77.9634	90.4048
rbio2.2	8.2601	15.7681	24.5573	34.7063	44.2470	54.8319	66.2440	78.0060	90.2942
rbio2.4	8.2737	15.4700	24.2293	34.3328	44.0759	54.9462	67.1456	78.9980	91.2474
rbio2.6	8.6603	16.0525	24.9207	35.1004	44.7972	55.5966	68.0189	79.7269	91.8074
rbio2.8	8.8784	16.4279	25.5171	35.8076	45.4564	56.4073	68.7109	80.3501	92.1843
rbio3.1	36.4408	47.3172	49.8115	52.4048	55.2432	60.0898	67.6257	77.2668	89.8288
rbio3.3	18.4187	33.8828	49.3290	61.1621	69.4909	76.0840	82.3558	88.7868	96.7126
rbio3.5	15.1663	29.2174	45.1930	58.6033	68.4000	76.6187	84.0868	90.6071	98.4630
rbio3.7	14.4717	28.1987	43.9258	57.8445	67.5738	75.9713	84.1076	91.2261	99.3106
rbio3.9	14.4742	28.0209	43.9021	57.5630	67.2161	75.9373	84.2706	91.6010	99.7624
rbio4.4	4.3338	8.0648	12.5693	18.7108	26.0661	35.7560	48.1534	62.9683	81.1557
rbio5.5	3.0208	5.4110	8.4883	12.8735	18.3762	26.4419	37.9083	53.0474	73.8949
rbio6.8	4.9172	9.1593	14.3950	21.3085	29.0712	39.2107	51.9503	66.9630	83.8937

However, rbio3.1, bior3.1 and bior3.3 always have bad reconstruction performance. When CR is greater than 35%, bior3.1 had the worst PRD. In addition, the PRDs in rbio3.5, rbio3.7 and rbio3.9 basis were poor either. It is not recommended to reconstruct the HS signal in these six wavelet basis.

In addition to the PRD performance, Table 2 reveals the similarity between the reconstructed HS signals and the original one under various wavelet basis. The results are similar to

but not equal with the PRDs in Table 1. The SSIM decreases with the increase of CR. In the range of 5%-60%, rbio5.5 has the best SSIM, more than 50%. On the other hand, rbio3.1 and bior3.1 had the worst similarity while rbio3.3, and rbio3.5, rbio3.7 and rbio3.9 don't possess satisfactory SSIM either. In addition, in a fixed CR, the required reconstruction times in the tested wavelet basis are roughly the same. Generally, the greater the CR, the shorter the reconstruction time.

TABLE 2. SSIM of various wavelet basis.

Wavelet basis	10%	20%	30%	40%	50%	60%	70%	80%	90%
hear	0.86	0.7598	0.6588	0.5342	0.4107	0.3106	0.1903	0.1053	0.0315
db2	0.9006	0.8173	0.7264	0.5998	0.4706	0.358	0.2346	0.131	0.0435
db3	0.9076	0.8363	0.748	0.6189	0.4938	0.3797	0.2521	0.1345	0.0489
db4	0.9136	0.8372	0.7536	0.6247	0.4981	0.3826	0.254	0.1419	0.0444
db5	0.9132	0.8404	0.753	0.6363	0.503	0.3857	0.2532	0.139	0.045
db6	0.9149	0.8459	0.7549	0.6343	0.503	0.3833	0.2515	0.1424	0.0474
db7	0.9168	0.8473	0.7592	0.6312	0.5042	0.3956	0.2583	0.1417	0.0482
db8	0.9146	0.8448	0.7535	0.6363	0.5123	0.3934	0.266	0.1436	0.045
db9	0.9172	0.847	0.7611	0.6325	0.4988	0.382	0.2509	0.1408	0.0464
db10	0.9136	0.8454	0.7543	0.6322	0.5046	0.3873	0.2531	0.1419	0.0483
sym2	0.9006	0.8173	0.7264	0.5998	0.4706	0.358	0.2346	0.131	0.0435
sym3	0.9076	0.8363	0.748	0.6189	0.4938	0.3797	0.2521	0.1345	0.0489
sym4	0.9149	0.8396	0.7533	0.6292	0.5058	0.3961	0.2631	0.1425	0.0501
sym5	0.9167	0.8436	0.7549	0.6321	0.5057	0.389	0.2523	0.1422	0.0484
sym6	0.9179	0.8447	0.754	0.6379	0.5151	0.3985	0.2667	0.1435	0.0511
sym7	0.918	0.8445	0.7602	0.6403	0.5071	0.4018	0.2607	0.1441	0.047
sym8	0.9179	0.8483	0.7579	0.6419	0.5152	0.3962	0.2685	0.1451	0.0519
coif1	0.9003	0.821	0.7284	0.6001	0.4766	0.3659	0.2466	0.1316	0.048
coif2	0.9126	0.8434	0.7575	0.6304	0.5077	0.3905	0.2631	0.1405	0.0509
coif3	0.9144	0.8475	0.7648	0.6345	0.5115	0.3959	0.2677	0.1423	0.0512
coif4	0.9175	0.8454	0.7679	0.6384	0.5103	0.3947	0.2691	0.145	0.051
coif5	0.9201	0.8469	0.7665	0.6413	0.5131	0.394	0.2654	0.1457	0.0493
bior1.1	0.86	0.7598	0.6588	0.5342	0.4107	0.3106	0.1903	0.1053	0.0315
bior1.3	0.9189	0.8495	0.768	0.6479	0.526	0.4037	0.255	0.1473	0.0475
bior1.5	0.9236	0.8557	0.7724	0.6516	0.5334	0.4128	0.2667	0.1551	0.0521
bior2.2	0.8874	0.8045	0.6883	0.5523	0.4251	0.3205	0.2144	0.1198	0.0494
bior2.4	0.9184	0.8555	0.7626	0.6412	0.5222	0.4075	0.2878	0.1652	0.0688
bior2.6	0.9257	0.8677	0.7833	0.6659	0.5554	0.4358	0.31	0.1803	0.0759
bior2.8	0.9292	0.8717	0.791	0.6764	0.5655	0.4459	0.3204	0.187	0.0796
bior3.1	0.742	0.5421	0.3816	0.2291	0.127	0.0726	0.0334	0.0129	0.005
bior3.3	0.8874	0.7717	0.6481	0.4841	0.3265	0.2267	0.14	0.078	0.037
bior3.5	0.9078	0.81	0.7005	0.5531	0.4103	0.2945	0.1981	0.1216	0.0574
bior3.7	0.9145	0.8277	0.7214	0.582	0.4462	0.3299	0.2266	0.1429	0.0661
bior3.9	0.9179	0.8349	0.7315	0.6043	0.4655	0.3493	0.2416	0.1549	0.0703
bior4.4	0.8923	0.8017	0.6876	0.5507	0.4293	0.3271	0.2176	0.113	0.0403
bior5.5	0.8515	0.7165	0.5807	0.4262	0.3074	0.2226	0.1324	0.0646	0.0189
bior6.8	0.915	0.8435	0.7515	0.6305	0.5118	0.3963	0.2685	0.1464	0.0542
rbio1.1	0.86	0.7598	0.6588	0.5342	0.4107	0.3106	0.1903	0.1053	0.0315
rbio1.3	0.8315	0.7124	0.6015	0.4705	0.3514	0.2591	0.1638	0.0921	0.0293
rbio1.5	0.8233	0.6953	0.5806	0.4484	0.327	0.2384	0.1514	0.0847	0.0274
rbio2.2	0.8674	0.7295	0.5988	0.4512	0.3269	0.2416	0.1594	0.0916	0.0332
rbio2.4	0.8676	0.7348	0.6052	0.4513	0.3255	0.2423	0.1561	0.0861	0.0296
rbio2.6	0.8617	0.7266	0.5947	0.4415	0.3192	0.2362	0.1502	0.0819	0.0278
rbio2.8	0.8582	0.7223	0.5861	0.4338	0.3131	0.2296	0.1457	0.0789	0.0264
rbio3.1	0.5081	0.4141	0.3852	0.3425	0.3133	0.2729	0.2046	0.1199	0.0409
rbio3.3	0.7152	0.5157	0.3422	0.2518	0.1928	0.152	0.1134	0.071	0.0228
rbio3.5	0.7607	0.5614	0.3714	0.2546	0.1855	0.139	0.099	0.0621	0.0185
rbio3.7	0.7719	0.5711	0.3824	0.2558	0.1844	0.1376	0.0949	0.0582	0.0165
rbio3.9	0.7723	0.5709	0.3829	0.2557	0.1841	0.1362	0.0919	0.0556	0.0155
rbio4.4	0.9257	0.8589	0.7784	0.6658	0.5379	0.42	0.2874	0.1637	0.0622
rbio5.5	0.945	0.9059	0.8457	0.7646	0.6674	0.5522	0.4037	0.2443	0.1029
rbio6.8	0.9179	0.8417	0.7498	0.6258	0.4932	0.3806	0.2549	0.1392	0.05

## B. PERFORMANCE ANALYSIS VERSUS RECONSTRUCTION ALGORITHMS

In this suite of experiments, 5 reconstruction algorithms are evaluated in terms of the PRD, SSIM and execution time. The sparsifying basis is fixed as db2, while the frame size is set as 1024 for fair comparison. The reconstruction performance of the compared algorithms is listed in Tables 3, 4 and 5. In addition, the PRDs are also plotted in Fig. 4 for visualized perception. As can be observed, different reconstruction

algorithms bring about different signal qualities. The results show that Irls has the best reconstruction PRD for almost every CR region. When CR is less than 35%, the PRD and SSIM performance of OMP algorithm are also more satisfactory than other counterparts. When CR is greater than 50%, BP algorithm can be used as an alternative in terms of PRD and SSIM. However, when CR is greater than 50%, PRDs and SSIMs of OMP and CoSaMP methods are unsatisfactory.

TABLE 3. PRD of various reconstruction algorithms.

Algorithms	10%	20%	30%	40%	50%	60%	70%	80%	90%
BP	6.0292	11.0188	16.3885	23.1710	31.1720	41.7657	52.9921	68.4678	85.5651
OMP	5.5380	9.5774	14.2397	21.8026	32.6202	48.2880	66.7271	90.3104	118.5109
CoSaMP	9.9755	12.1141	15.2541	20.6488	29.7681	47.8450	68.3914	91.0147	112.0554
Irls	3.5618	6.7443	10.6787	16.1072	23.5149	33.8117	45.5713	62.5557	84.3012
SP	10.3353	12.5627	15.7478	20.7660	29.0758	42.2533	58.2479	80.2740	104.0563

TABLE 4. SSIM of various reconstruction algorithms.

Algorithms	10%	20%	30%	40%	50%	60%	70%	80%	90%
BP	0.9008	0.8135	0.7176	0.5984	0.4746	0.3478	0.2350	0.1270	0.0410
OMP	0.9113	0.8446	0.7564	0.6372	0.4652	0.2987	0.1814	0.0945	0.0374
CoSaMP	0.8323	0.7882	0.7200	0.6099	0.4575	0.3141	0.1806	0.1548	0.0388
IRLS	0.9395	0.8834	0.8072	0.7098	0.5664	0.4123	0.2847	0.1557	0.0441
SP	0.8216	0.7787	0.6980	0.5996	0.4597	0.3100	0.2026	0.1174	0.0486

TABLE 5. Reconstruction time of various reconstruction algorithms.

Algorithms	10%	20%	30%	40%	50%	60%	70%	80%	90%
BP	11.4765	9.6877	8.0554	6.7669	5.4703	4.2137	3.0412	2.5191	2.005
OMP	857.9601	580.165	376.1595	225.5641	123.6176	55.9108	20.9316	6.9083	1.0691
CoSaMP	323.3513	221.0618	157.3298	99.7399	52.2744	21.1266	9.5246	3.4006	0.7567
Irls	671.3869	725.3193	545.2352	394.9726	263.0556	155.5577	84.3698	37.3615	11.579
SP	187.9845	133.1603	80.1687	49.5136	22.7025	11.9847	5.5953	2.2019	0.5261

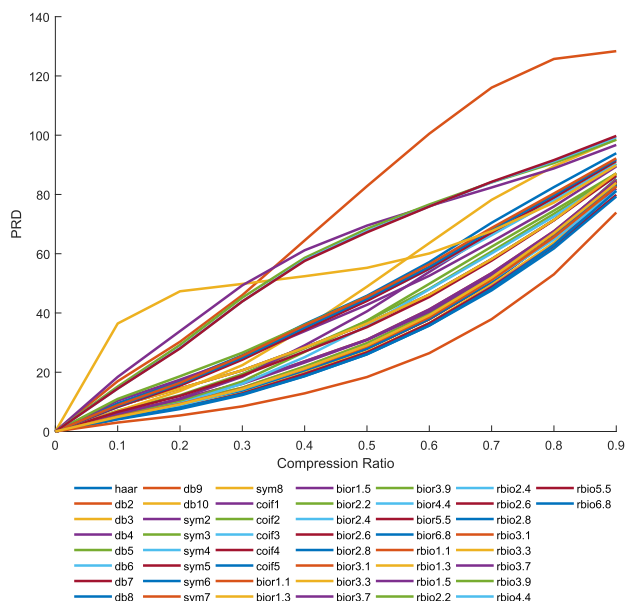


FIGURE 3. PRD versus different wavelet basis.

The execution times of the reconstruction algorithms are very different from each other, as listed in Table 5. The BP generally acts as the most efficient reconstruction algorithm, while the operation time of SP is also relatively shorter. However, Irls requires the longest operation time. In addition, OMP and CoSaMP don't have remarkable advantageous in each region either.

The SSIMs between the original signal and the reconstructed signals are also calculated. The results are listed

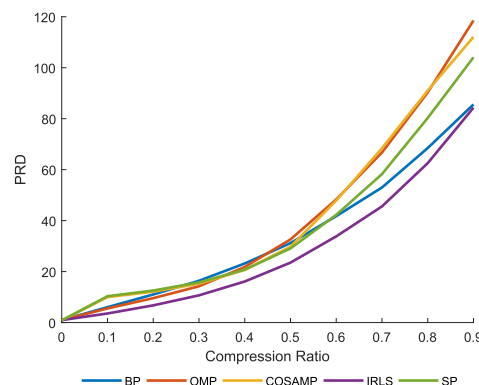


FIGURE 4. PRD in different reconstruction algorithms.

in Table 4. The Irls algorithm has the highest SSIM, it almost reaches up to 95.8%. The SSIMs obtained by CoSaMP and SP algorithms are relatively lower.

Referring to the aforementioned experimental results, we can conclude that the Irls is the best reconstruction algorithm in terms of signal quality, but it takes the longest time to be executed. The BP algorithm has better compromise in terms of execution efficiency and reconstruction quality. In addition, when CR is greater than 50%, SP may also be considered. On the other hand, if reconstruction quality is a priority, the Irls algorithm is recommended.

C. PERFORMANCE ANALYSIS VERSUS FRAME SIZE

This section describes the impact of frame size to the signal reconstruction quality. The BP is fixed as the

TABLE 6. PRD of various frame sizes.

Frame size	10%	20%	30%	40%	50%	60%	70%	80%	90%	
256	3.9173	6.5206	12.2285	17.8231	24.1271	34.5728	46.0472	59.7709	71.7824	93.0173
512	3.8357	6.3627	11.3656	16.8066	23.6679	32.6652	42.7463	56.3965	69.7876	87.3390
768	3.6937	6.0196	10.9525	16.2349	23.1605	31.6383	41.5339	53.3578	69.0209	85.4739
1024	3.6771	6.0420	10.6815	16.2119	22.9602	31.7885	40.9209	54.2869	68.0594	84.8560
2048	3.7628	6.0938	11.0824	16.3796	23.2359	31.2115	41.5065	53.1092	67.7314	86.2354
3072	3.7969	6.2078	11.0417	16.5752	23.1376	31.3892	41.2880	53.5705	68.4010	85.9643
4096	3.7792	6.2777	10.9930	16.3029	23.2115	31.6739	41.8515	53.4386	68.3121	86.4659

TABLE 7. SSIM of different frame sizes.

Frame size	10%	20%	30%	40%	50%	60%	70%	80%	90%
256	0.9084	0.8198	0.7494	0.6900	0.5080	0.3775	0.2157	0.1594	0.0332
512	0.9083	0.8225	0.7165	0.6362	0.5006	0.3715	0.2332	0.1389	0.0456
768	0.8972	0.8136	0.7215	0.6050	0.4804	0.3500	0.2397	0.1155	0.0412
1024	0.8997	0.8152	0.7163	0.6117	0.4666	0.3628	0.2288	0.1248	0.0398
2048	0.8902	0.7959	0.6965	0.5780	0.4580	0.3317	0.2170	0.1191	0.0328
3072	0.8887	0.7953	0.6937	0.5752	0.4517	0.3296	0.2192	0.1141	0.0368
4096	0.8830	0.7956	0.6986	0.5720	0.4441	0.3220	0.2098	0.1148	0.0336

TABLE 8. Reconstruction time of different frame sizes.

Frame size	10%	20%	30%	40%	50%	60%	70%	80%	90%
256	0.6601	0.5998	0.5320	0.4989	0.4970	0.4431	0.4080	0.3785	0.3464
512	4.4160	4.3695	3.3838	3.2022	2.9873	2.5821	2.4756	2.3830	2.2862
768	10.6617	9.8293	8.9020	8.2075	7.4481	6.5044	6.0479	5.5575	5.3750
1024	20.0670	18.8880	16.7226	16.0283	14.2595	13.0489	12.3528	11.6003	10.3172
2048	119.7231	112.4036	93.7834	88.6368	79.8995	74.2527	70.0138	67.1209	57.5594
3072	342.0246	305.2268	273.8622	242.2887	218.3298	194.7132	184.6064	177.3049	150.5862
4096	723.5457	632.7409	597.6457	508.5414	462.6418	429.7729	384.3703	355.2914	299.8624

reconstruction algorithm. The tested frame sizes range from 256 to 4096. The results are listed in Tables 6-8, while the PRDs are also visualized demonstrated in Fig. 5. As indicated by these results, at different frame size, PRD increases with CR. On the same CR, the reconstructed PRDs with frame size of 256 and 512 are relatively poorer. Table 7 compares the similarity between the reconstructed signals with the original one. It is revealed that similar SSIMs have been obtained in terms of various frame sizes. However, a signal with a frame size of 256 has a better SSIM than the other frame sizes. Such an observation is a bit different from that

derived from the PRD values in Table 6. Table 8 shows the relationship between reconstruction time and frame size. It is obviously that under the same CR, the longer the signal frame, the longer the operation time.

D. DISCUSSIONS

The aforementioned experiments discuss the application of CS for HS acquisition, exploring the performance in terms of 5 reconstruction algorithms, 52 wavelet basis and different frame sizes. Then corresponding observations are illustrated.

Among the five reconstruction algorithms, the Irls has the best reconstruction quality, but also has the longest reconstruction time. It is suggested that Irls algorithm can be selected when the requirements of reconstruction quality are of higher superiority. On the other hand, BP and SP algorithms can make a compromise between execution time and reconstruction quality at different compression levels. Observing the performance indicators in terms of wavelet basis, it is shown that rbio5.5 is the best wavelet basis. The rbio5.5 can be used for practical applications, or act as a benchmark for the future research in term of sparsifying basis for CS acquisition of HS. In the analysis of frame size, it is concluded that the frame size from 256 to 4096 has little influence on the reconstruction quality. The reconstructed signals from different frame sizes have indistinctive difference in terms of PRD and SSIM.

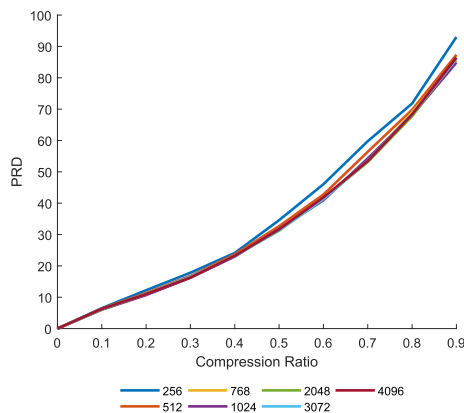


FIGURE 5. PRD in different frame sizes.



Referring to the presented data records, for practical applications owing different types of requirements, the users can choose suitable combinations of wavelet basis, reconstruction algorithm and the frame size. In addition, these results can also be used as benchmarks for academic research of HS acquisition using CS. For example, if we want to develop a suitable reconstruction algorithm, the Irls should be compared in terms of reconstruction quality while the executive time should be compared with BP. In this scenario, the developed algorithm can be declared satisfactory when it has superiorities in both dimensions.

## V. CONCLUSION

In this paper, the acquisition of heart sound signals by compressed sensing is comparatively studied. Amounts of experiments have been carried out and the results are analyzed in detail. Experimental results show that rbio5.5 is considered being a satisfactory wavelet basis for heart sound acquisition, while Irls gives best reconstruction quality and BP algorithm has good efficiency. In addition, we also analyze the impact of the frame size, and conclude that the frame size has little effect on the reconstruction accuracy. The involved conclusions in terms of sparsifying basis, reconstruction algorithms can be used as benchmarks for future academic scientific research, and the experimental data records are also believed being beneficial for practical applications.

## REFERENCES

- [1] S. Kaptoge, L. Pennells, D. De Bacquer, M. T. Cooney, M. Kavousi, G. Stevens, L. M. Riley, S. Savin, T. Khan, and S. Altay, "World health organization cardiovascular disease risk charts: Revised models to estimate risk in 21 global regions," *Lancet Global Health*, vol. 7, no. 10, pp. e1332–e1345, 2019.
- [2] S.-L. Chen, H.-Y. Lee, C.-A. Chen, C.-C. Lin, and C.-H. Luo, "A wireless body sensor network system for healthcare monitoring application," in *Proc. IEEE Biomed. Circuits Syst. Conf.*, Nov. 2007, pp. 243–246.
- [3] W. Wang, J. Chen, J. Wang, J. Chen, and Z. Gong, "Geography-aware inductive matrix completion for personalized point of interest recommendation in smart cities," *IEEE Internet Things J.*, to be published.
- [4] W. Wang, J. Chen, J. Wang, J. Chen, J. Liu, and Z. Gong, "Trust-enhanced collaborative filtering for personalized point of interests recommendation," *IEEE Trans. Ind. Inf.*, to be published.
- [5] X. Wang, L. Wan, M. Huang, C. Shen, and K. Zhang, "Polarization channel estimation for circular and non-circular signals in massive MIMO systems," *IEEE J. Sel. Topics Signal Process.*, vol. 13, no. 5, pp. 1001–1016, Sep. 2019.
- [6] L. Wan, X. Kong, and F. Xia, "Joint range-Doppler-angle estimation for intelligent tracking of moving aerial targets," *IEEE Internet Things J.*, vol. 5, no. 3, pp. 1625–1636, Jun. 2018.
- [7] F. Wen, J. Shi, and Z. Zhang, "Joint 2D-DOD, 2D-DOA and polarization angles estimation for bistatic EMVS-MIMO radar via PARAFAC analysis," *IEEE Trans. Veh. Technol.*, to be published.
- [8] J. Chen, J. Xing, L. Y. Zhang, and L. Qi, "Compressed sensing for electrocardiogram acquisition in wireless body sensor network: A comparative analysis," *Int. J. Distrib. Sensor Netw.*, vol. 15, no. 7, Jul. 2019, Art. no. 155014771986488.
- [9] L. Wan, L. Sun, X. Kong, Y. Yuan, K. Sun, and F. Xia, "Task-driven resource assignment in mobile edge computing exploiting evolutionary computation," *IEEE Wireless Commun.*, vol. 26, no. 6, pp. 94–101, Dec. 2019.
- [10] H. Wang, L. Wan, M. Dong, K. Ota, and X. Wang, "Assistant vehicle localization based on three collaborative base stations via SBL-based robust DOA estimation," *IEEE Internet Things J.*, vol. 6, no. 3, pp. 5766–5777, Jun. 2019.
- [11] R. Cavallari, F. Martelli, R. Rosini, C. Buratti, and R. Verdone, "A survey on wireless body area networks: Technologies and design challenges," *IEEE Commun. Surveys Tuts.*, vol. 16, no. 3, pp. 1635–1657, Feb. 2014.
- [12] D. Craven, B. Mcginley, L. Kilmartin, M. Glavin, and E. Jones, "Compressed sensing for bioelectric signals: A review," *IEEE J. Biomed. Health Inform.*, vol. 19, no. 2, pp. 529–540, Mar. 2015.
- [13] Z. Zhang, T.-P. Jung, S. Makeig, and B. D. Rao, "Compressed sensing of eeg for wireless telemonitoring with low energy consumption and inexpensive hardware," *IEEE Trans. Biomed. Eng.*, vol. 60, no. 1, pp. 221–224, Jan. 2013.
- [14] Y. Zhang, Q. He, Y. Xiang, L. Y. Zhang, B. Liu, J. Chen, and Y. Xie, "Low-Cost and confidentiality-preserving data acquisition for Internet of multimedia Things," *IEEE Internet Things J.*, vol. 5, no. 5, pp. 3442–3451, Oct. 2018.
- [15] J.-X. Chen, Z.-L. Zhu, C. Fu, H. Yu, and L.-B. Zhang, "Gyrator transform based double random phase encoding with sparse representation for information authentication," *Opt. Laser Technol.*, vol. 70, pp. 50–58, Jul. 2015.
- [16] X. Chai, H. Wu, Z. Gan, Y. Zhang, Y. Chen, and K. W. Nixon, "An efficient visually meaningful image compression and encryption scheme based on compressive sensing and dynamic LSB embedding," *Opt. Lasers Eng.*, vol. 124, Jan. 2020, Art. no. 105837.
- [17] X. Chai, X. Fu, Z. Gan, Y. Zhang, Y. Lu, and Y. Chen, "An efficient chaos-based image compression and encryption scheme using block compressive sensing and elementary cellular automata," *Neural Comput. Appl.*, pp. 1–28, Nov. 2018. [Online]. Available: <https://link.springer.com/article/10.1007/s00521-018-3913-3>
- [18] J. Chen, Y. Zhang, and L. Y. Zhang, "On the security of optical ciphers under the architecture of compressed sensing combining with double random phase encoding," *IEEE Photon. J.*, vol. 9, no. 4, pp. 1–11, Aug. 2017.
- [19] J. K. Pant and S. Krishnan, "Compressive sensing of electrocardiogram signals by promoting sparsity on the second-order difference and by using dictionary learning," *IEEE Trans. Biomed. Circuits Syst.*, vol. 8, no. 2, pp. 293–302, Apr. 2014.
- [20] Z. Zhang, T.-P. Jung, S. Makeig, Z. Pi, and B. D. Rao, "Spatiotemporal sparse Bayesian learning with applications to compressed sensing of multichannel physiological signals," *IEEE Trans. Neural Syst. Rehabil. Eng.*, vol. 22, no. 6, pp. 1186–1197, Nov. 2014.
- [21] L. F. Polania and K. E. Barner, "Multi-scale dictionary learning for compressive sensing ECG," in *Proc. IEEE Digit. Signal Process. Signal Process. Edu. Meeting (DSP/SPE)*, Aug. 2013, pp. 36–41.
- [22] Z. Zhang, X. Liu, S. Wei, H. Gan, F. Liu, Y. Li, C. Liu, and F. Liu, "Electrocardiogram reconstruction based on compressed sensing," *IEEE Access*, vol. 7, pp. 37228–37237, 2019.
- [23] J. K. Pant and S. Krishnan, "Performance of compressive sensing for the reconstruction of different QRS pulses in ECG signals," in *Proc. 39th Annu. Int. Conf. IEEE Eng. Med. Biol. Soc. (EMBC)*, Jul. 2017, pp. 825–828.
- [24] A. Majumdar and R. K. Ward, "Energy efficient EEG sensing and transmission for wireless body area networks: A blind compressed sensing approach," *Biomed. Signal Process. Control*, vol. 20, pp. 1–9, Jul. 2015.
- [25] A. M. R. Dixon, E. G. Allstot, D. Gangopadhyay, and D. J. Allstot, "Compressed sensing system considerations for ECG and EMG wireless biosensors," *IEEE Trans. Biomed. Circuits Syst.*, vol. 6, no. 2, pp. 156–166, Apr. 2012.
- [26] E. Sejdic and L. F. Chaparro, "Recovering heart sounds from sparse samples," in *Proc. 38th Annu. Northeast Bioeng. Conf. (NEBEC)*, Mar. 2012, pp. 107–108.
- [27] X. Cheng, S. Feng, Y. Li, and G. Gui, "Research on parallel compressive sensing and application of multi-channel synchronous acquisition of heart sound signals," *IEEE Access*, vol. 7, pp. 30033–30041, 2019.
- [28] H. Mamaghanian, N. Khaled, D. Atienza, and P. Vanderghyest, "Structured sparsity models for compressively sensed electrocardiogram signals: A comparative study," in *Proc. IEEE Biomed. Circuits Syst. Conf. (BioCAS)*, Nov. 2011, pp. 125–128.
- [29] G. Da Poian, R. Bernardini, and R. Rinaldo, "Gaussian dictionary for compressive sensing of the ECG signal," in *Proc. IEEE Workshop Biometric Meas. Syst. Secur. Med. Appl. (BIOMS)*, 2014, pp. 80–85.
- [30] Z. Zhang, S. Wei, D. Wei, L. Li, F. Liu, and C. Liu, "Comparison of four recovery algorithms used in compressed sensing for ECG signal processing," in *Proc. Comput. Cardiol. Conf. (CinC)*, 2016, pp. 401–404.

- [31] N. Zhang, C. Zhang, and Y. Li, "The analysis of the anomaly characteristic of heart sound based on heart sounds segmentation algorithm," in *Proc. Int. Conf. Comput. Sci. Service Syst.*, Aug. 2012, pp. 1339–1342.
- [32] V. N. Varghees and K. Ramachandran, "A novel heart sound activity detection framework for automated heart sound analysis," *Biomed. Signal Process. Control*, vol. 13, pp. 174–188, Sep. 2014.
- [33] X. Cheng, Y. Ma, C. Liu, X. Zhang, and Y. Guo, "An introduction to heart sounds identification technology," *SCIENTIA SINICA Inf.*, vol. 42, no. 2, pp. 237–251, 2012.
- [34] I. D. Irawati and E. M. Dewi, "Comparing on sparse heart sound recovery algorithms," in *Proc. Int. Seminar Intell. Technol. Appl. (ISITIA)*, Jul. 2016, pp. 111–116.



**SHUANG SUN** was born in Changchun, China. She received the bachelor's degree in measurement and control technology and instrumentation from Northeast Petroleum University. She is currently pursuing the master's degree in biomedical information engineering with Northeastern University, Shenyang, China. Her research interest includes ECG signal processing and compressed sensing for biological signals.



**JIAZHU XING** was born in Dandong, China. He received the bachelor's degree major in computer science and technology from Northeastern University, Shenyang, in 2016, where he is currently pursuing the master's degree in biomedical engineering. His research interests include compressed sensing and over-complete dictionary.

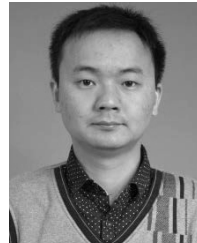


**ZHENG ZHOU** received the bachelor's degree in electronic science and technology from the University of Electronic Science and Technology of China, Chengdu, China, in 2017. He is currently pursuing the Ph.D. degree with the Department of Computer and Information Science, University of Macau, Macau. His research interests include pattern recognition, machine learning, and sparse signal processing.



**WEI WANG** (Member, IEEE) received the B.Sc. degree in electronic information science and technology from Shenyang University, in 2012, and the Ph.D. degree in software engineering from the Dalian University of Technology, in 2018.

He is currently a Postdoctoral Fellow with the University of Macau, Taipa, Macau. He has authored/coauthored over 30 scientific articles in international journals and conferences, i.e., IEEE TRANSACTIONS ON BIG DATA, the IEEE TRANSACTIONS ON EMERGING TOPICS IN COMPUTING, the IEEE TRANSACTIONS ON HUMAN-MACHINE SYSTEMS, and WWW. His research interests include computational social science, data mining, and mobile social networks. He was a recipient of the Best Paper Award of the IEEE International Conference on Ubiquitous Intelligence and Computing, in 2014. He has served as a multiple conference/journal reviewers, including the *IEEE Wireless Communication Magazine*, IEEE TBD, IEEE TETC, IJCAI, and WWW.



**JUNXIN CHEN** received the B.Sc., M.Sc., and Ph.D. degrees in communications engineering from Northeastern University, Shenyang, China, in 2007, 2009, and 2016, respectively. He is currently an Associate Professor with the College of Medicine and Biological Information Engineering, Northeastern University, and the Department of Computer and Information Science, University of Macau, Macau. His research interests include biosignal processing, compressive sensing, security, and privacy.

...